Research Paper

Time-domain transient fluorescence spectroscopy for thermal characterization of polymers

Hao Wu[a,b], Kai Cai[b], Hongtao Zeng[a,b], Wensheng Zhao[a,b], Danmei Xie[a,b], Yanan Yue[a,b,c,*], Yangheng Xiong[a,b], Xin Zhang[c]

[a] *Key Laboratory of Hydraulic Machinery Transients (Wuhan University), MOE, 430072, China*
[b] *School of Power and Mechanical Engineering, Wuhan University, Wuhan, Hubei 430072, China*
[c] *Department of Mechanical Engineering, Boston University, Boston, MA 02215, USA*

ABSTRACT

In this work, a time-domain fluorescence spectroscopy technique is developed to characterize thermophysical properties of polymers. The method is based on fluorescence thermometry of materials under periodic pulse heating. In the characterization, a continuous laser (405 nm) is modulated with adjustable periodic heating and fluorescence excitation. The temperature rise at sample surface due to laser heating is probed from simultaneous fluorescence spectrum. Thermal diffusivity can be determined from the relationship between normalized temperature rise and the duration of laser heating. To verify this technique, thermal diffusivity of a polymer material (PVC) is characterized as $1.031 \times 10^{-7}\,\mathrm{m^2/s}$, agreeing well with reference data. Meanwhile, thermal conductivity can be obtained by the hot plate method. Then, both steady and unsteady thermophysical properties are available. Quenching effect of fluorescence signal in our measurement can be ignored, as validated by longtime laser heating experiments. The uncertainty induced by uniformity of laser heating is negligible as analyzed through numerical simulations. This non-destructive fluorescence-based technique does not require exact value about laser absorption and calibration experiment for temperature coefficient of fluorescence signals. Considering that most polymers can excite sound fluorescence signal, this method can be well applied to thermal characterization of polymer-based film or bulk materials.

1. Introduction

In recent years, polymer-based materials have been studied extensively [1–4], and have shown great potentials in biomedical [5], photovoltaic solar cells [6], supercapacitors [7], LEDs [8] and so on [9]. Thermal conductivity and thermal diffusivity are important thermophysical parameters which determine steady and unsteady thermal transport performance. Thus, accurate measurement of these parameters is the key to the successful thermal design of polymer-based heat dissipation applications. Most polymer materials are poor in thermal transport, and thus extremely thin structures are usually used in electronics, not many techniques are available for thermal characterization. To date, a few works have been reported for successful characterization of polymers. Kim et al. used differential 3ω method to measure thermal conductivity of an amorphous-structured polymer as 1.5 W/m K [10]. In Lee et al.'s work, a modified hot wire method was employed to explore the thermal conductivity enhancement of polymer composites filled with hybrid filler [11].

The above referenced techniques are joule heating-based methods. Meanwhile, various optical techniques have been applied to polymer's characterizations. Song et al. studied thermal conductivity of an epoxy-graphene composites as 1.53 W/m K by laser flash method [12,13]. In another work, Wang et al. used time-domain thermoreflectance (TDTR) method to measure thermal conductivity of polymer fibers [14]. The TDTR method coupled with ultra-fast laser offers a superior temporal resolution, however, has drawbacks on the complexity in system operation and data analysis. As a spectroscopy method, Raman spectrum has been widely used for temperature probing and thermal characterization in recent years [15–18]. Generally, Raman thermometry is for steady state thermal measurement, e.g., the first report of superior thermal conductivity of graphene [19]. Recently, Raman thermometry has been successfully extended to transient measurement based on periodic laser heating and Raman excitation. The characterized thermal parameter is not limited to thermal conductivity but also thermal diffusivity [15,16,20]. However, when it comes to polymers, Raman scattering is not as significant as other crystalline structures. Thus, it is

not a good option to use Raman thermometry on characterization of polymers.

Fluorescence is another commonly used spectroscopy technique which also possess strong temperature dependent property. Moreover, fluorescence signal can be easily detected from polymers [21–24]. With high sensitivity and short response time ($< 10^{-9}$ s) [25], fluorescence thermometry has been used in thermal imaging and temperature probing [26–29]. Here are some examples: Ivan et al. measured the temperature of glass-ceramic material based on its fluorescence emission [30]. Donner et al. used green fluorescent proteins as the thermal probe for intracellular temperature mapping [31]. Yarimaga et al. employed conjugated polymers as temperature sensor in an integrated circuit chip [32]. Recently, our group developed a steady-state electrical-heating fluorescence-sensing (SEF) technique for thermal conductivity measurement of materials [33], showing that fluorescence signal can be well applied to thermal characterizations. In this paper, we extend above technique to the transient thermal measurement, and establish a novel technique termed time-domain transient fluorescence spectroscopy to characterize thermal diffusivity of materials.

2. Physical model and experimental principle

As shown in Fig. 1(a), the sample is heated and excited by multiple laser pulses (or a continuous laser with modulated mode). The fluorescence signal is collected during the laser heating period. The sample is placed on a heat sink in a vacuum chamber to eliminate convection heat loss. The schematic of thermal transport is presented in Fig. 1(b). If the heating pulse is very short compared with heat diffusion time of the sample, the thermal transport is only confined within a very thin layer near sample surface. A semi-infinite model is applicable to describe the temperature evolution during laser heating, and the temperature rise at sample surface can be derived as:

$$T(t) = \frac{2q_0\sqrt{\alpha t/\pi}}{k}\exp(-x^2/4\alpha t) - \frac{q_0 x}{k}erfc(x/2\sqrt{\alpha t}) + T_0 \tag{1}$$

where α is thermal diffusivity, k is thermal conductivity, q_0 is heat flux density induced by laser heating, T_0 is room temperature, x is the distance from any cross section to the surface, $erfc$ is the complementary error function. The sample is thick enough to ensure that the bottom of the sample stays at room temperature. It is shown in this model that α can be obtained from temperature rise against heating time.

Fluorescence signal is temperature dependent in terms of photon density (signal intensity), photon frequency (wavelength), photon decay (lifetime). Among various temperature indicators, fluorescence

intensity is strong and features high sensitivity for temperature probing. Thus, based on excited fluorescence intensity, the temperature of sample surface can be obtained under pulse laser heating. As shown in Fig. 2(a), the pulse laser consists of an excitation period (t_e) followed by a relaxation period (t_r). Under laser heating, rising temperature of the sample causes the decrease of fluorescence intensity. During the off-duty period (much longer time), the sample is fully cooled down to room temperature. Fig. 2(b) shows selected laser pulses under various excitation periods. The temperature rise under different laser heating period can be obtained by accumulating fluorescence signal exited from all pulses. The fluorescence spectrum in one period of heating-cooling cycle is shown in Fig. 2(c). As excitation times (t_e) is increased, fluorescence intensity is decreased. Fig. 2(d) shows significant decrease in fluorescence intensity for sample temperature from 30 °C to 70 °C.

The heating power is always required in most characterization techniques. In this measurement, the heat source q_0 (laser absorption) is yet hard to define and characterize, especially for an unknown material. To avoid such uncertainty, a normalized temperature rise: $T(t)^* = [T(t) - T_0]/(T_m - T_0)$ is defined, where T_0 is room temperature and T_m is the maximum temperature rise. Meanwhile, the temperature coefficient is not necessary for thermal diffusivity measurement. By defining $F(t) = 2\sqrt{\alpha t/\pi}\exp(-x^2/4\alpha t) - x\cdot erfc(x/2\sqrt{\alpha t})$, the normalized temperature rise is derived as: $T(t)^* = [t_m\cdot\int_0^x\int_0^t F(t)]/[t\cdot\int_0^x\int_0^{t_m} F(t)]$, where t_m is the maximum heating time. α can be obtained from the normalized temperature rise against heating time. To test this model, a polymer material (poly vinyl chloride, PVC) with known thermal properties is employed for verification. PVC is one of the most widely produced synthetic polymers [34]. Its thermal conductivity is around 0.16 W/m K [35]. Most importantly, PVC can excite strong fluorescence signal with desirable temperature dependence, as shown in Fig. 2(c) and (d).

3. Results and discussion

3.1. Experimental verification and results analysis

In the measurement, the PVC is placed in a vacuum chamber to eliminate convection heat loss. The PVC bottom is attached on a copper heat sink. A continuous semiconductor laser (150 mW) with 405 nm wavelength is modulated with adjustable pulse duration. Different from other measurements with two-laser configurations, only one laser in the measurement is employed as the heating and fluorescence excitation source. Excitation spectra are collected by a fluorescence spectrometer (HR2000+, Ocean Optics). The fluorescence signals between 450 nm
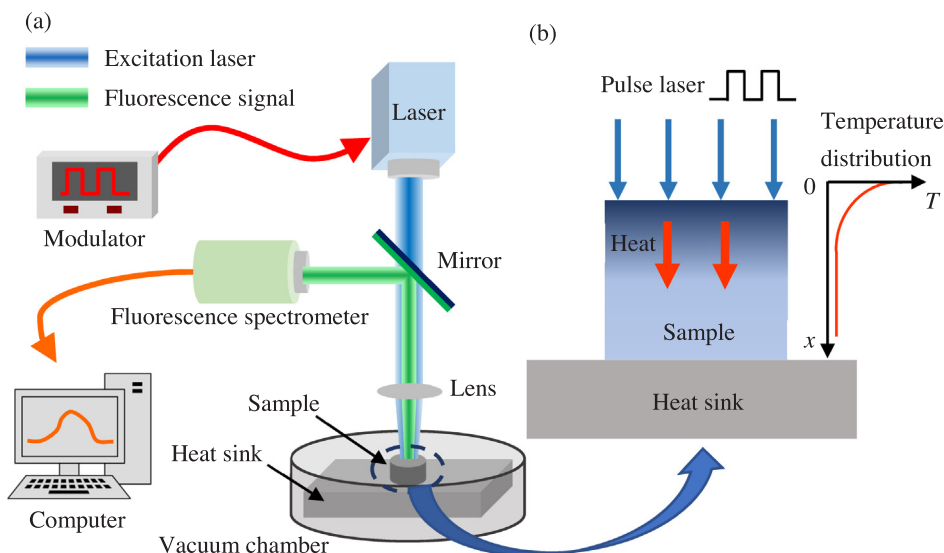

Fig. 1. (a) The schematic of time-domain transient fluorescent technique. A continuous laser is modulated by an electric-optical modulator to generate variable square pulse. The laser beam is focused on the sample for both photon heating and fluorescence excitation. Fluorescence signal is collected by a spectrometer for temperature measurement. (b) The schematic of thermal transport in polymers. For a short period of laser heating, thermal transport is confined within a layer close to the sample surface. The heat sink with large heat capacity ensures that the bottom of the sample keeps at room temperature. The vacuum condition of the sample eliminates the heat convection effect.
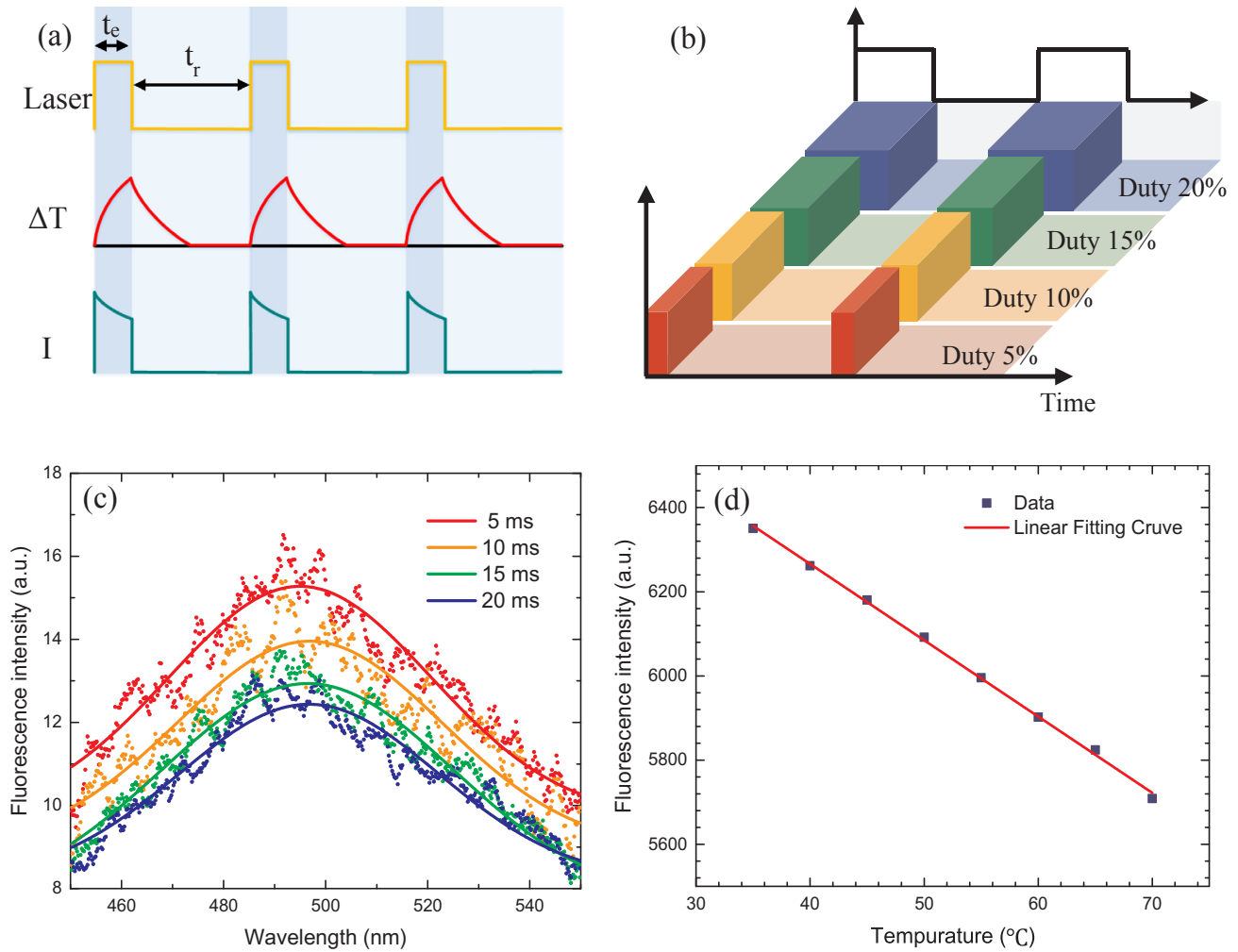
Fig. 2. (a) Thermal response of the sample heated by a pulsed laser, consisting of exciting periods (t_e) and off-duty periods (t_r). The temperature rises quickly and the fluorescence intensity drop simultaneously when the laser is on (not to scale). (b) Schematic of laser heating with different excitation periods (t_e). (c) Typical fluorescence spectra with various heating periods. It shows that fluorescence intensity is decreased with excitation time (t_e). (d) The relationship between fluorescence intensity and temperature.

and 550 nm exhibit one major peak at 491 nm. The pulse frequency of the laser is 10 Hz for all measurements. The heating time (t_e = duty time/frequency) is from 1 ms to 20 ms in one cycle with adjustable duty ratio [$t_e/(t_e + t_r)$] from 1% to 20%.

Fig. 3(a) shows the relationship between fluorescence intensity and heating time. A decreasing trend for fluorescence intensity is observed in a short period time (20 ms), illustrating the temperature rise under laser heating. According to the linear relationship between fluorescence intensity and temperature rise ($I \propto T$) in the calibration, the normalized temperature rise of PVC is a function of fluorescence intensity by: $T(t)^* = [I(t) - I_0]/[I_m - I_0]$, where $I(t)$ is the fluorescence intensity at different heating time, I_0 and I_m are fluorescence intensity at room temperature and at the longest heating time (20 ms) respectively. The normalized temperature rise is shown in Fig. 3(b). For the low thermal conductivity and thermal diffusivity of polymer material, obvious temperature rise can be obtained within a short heating period. To minimize heat accumulation, the first heating-cooling cycle is adopted to extract fluorescence signal in our measurement. Based on the above model, the thermal diffusivity of PVC is obtained as 1.031×10^{-7} m^2/s, which is in good agreement with reported values characterized by laser flash technique (1.095×10^{-7} m^2/s) and hot wire technique (0.985×10^{-7} m^2/s) [13].

For steady-state thermal transport analysis, a hot plate method is used to measure thermal conductivity of our PVC sample [36,37]. As is

shown in Fig. 4(a), the PVC sample is placed between a hot plate and a water-cooled plate. Different from ideal adiabatic environment, the distributions of heat flux are shown in Fig. 4(b). In the experiment, heat transferred in one direction at the measured region of 200 mm × 200 mm. The thermal conductivity is given by: $k = Ql/2A(T_h - T_c)$. Where Q is the heating power, l is thickness of PVC, A is heating area of the plates. ($T_h - T_c$) is the temperature difference between hot plate and cold plate. Thermal conductivity is characterized as 0.19 W/m K. Combined with the thermal diffusivity result, the volumetric heat capacity (ρc_p) is calculated as 1843 kJ/m^3 K, which is a little higher than the reference value (about 1634 kJ/m^3 K at 20 °C) [38]. Considering that our measurement temperature is above 20 °C and the higher temperature may induce the increasing of volumetric heat capacity [13,39], the characterization result for volumetric heat capacity is reasonable.

3.2. Quenching effect and uniformity of laser heating

Quenching effect should be considered in most fluorescence experiment. The fluorescence quenching effect refers to a complex process of intensity decreasing caused by various factors [40–42]. In our measurement, it is required to minimize such effect. In our measurement, the power of laser excitation is set as a minimum value to avoid too much heat accumulation and temperature rise. To confirm this, it is
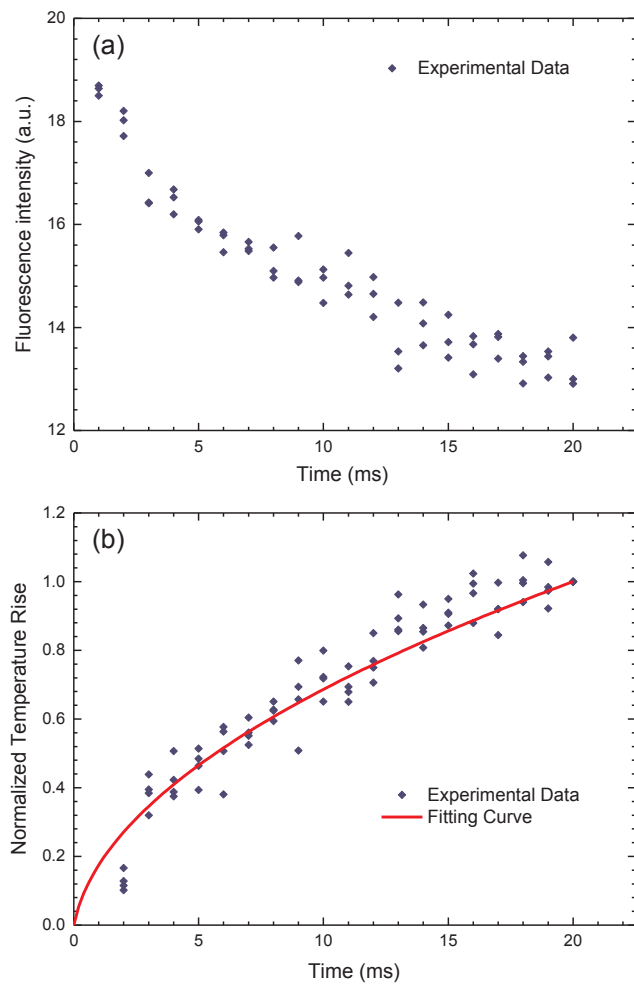
Fig. 5. Fluorescence spectrum of PVC under longtime irradiation to analyze quenching effect. The laser pulse is repeated 20 times to compare with the first time irradiation. It shows that the 20th spectrum (blue line) has dropped only 1.6% in intensity compared with the 1st spectrum (red line). (For interpretation of the references to colour in this figure legend, the reader is referred to the web version of this article.)

non-uniform heating effect on characterization result, a numerical simulation is conducted. In the simulation, all parameters about the sample and boundary conditions are consistent with experiments. The simulation results of normalized temperature rise with heating period are shown in Fig. 6. The temperature rise in the profile is an averaged value across the whole heating area of sample surface in both uniform and Gaussian irradiation. It is shown that the curve of Gaussian laser beam is almost overlap with that of uniform laser heating. It is feasible to apply our analytical solution derived from uniform laser heating to this thermal characterization.

3.3. Uncertainty analysis and extended measurement capacity

The experimental uncertainty is mainly introduced by heat loss and measurement errors. Since our measurement is conducted in a vacuum chamber, the convection heat loss of the simple surface can be neglected. The heat radiation is calculated by Stefan–Boltzmann law: $\Phi = \varepsilon \sigma A(T^4 - T_0^4)$, where ε is emissivity, σ is blackbody radiation constant: $5.67 \times 10^{-8}\,\mathrm{W/(m^2\,K^4)}$, A is sample surface area, T is surface temperature, T_0 is room temperature. Taking 1 for emissivity ε, it is calculated that the radiation heat loss is 0.23 mW for the highest temperature case which is negligible compared with laser heating power.

Aside from heat loss effect, the measurement uncertainty is mainly from fluorescence signal processing. As is shown in Fig. 2(d), the slope

Fig. 3. (a) The relationship between fluorescence intensity and heating time. The intensity is decreased with laser heating time (pulse duration). (b) The normalized temperature rise and the fitting curve for measuring the thermal diffusivity as $1.031 \times 10^{-7}\,\mathrm{m^2/s}$.

repeated 20 times for laser irradiation. The 1st spectrum and 20th spectrum are shown in Fig. 5. Only 1.6% for the intensity drop is observed. It can be concluded that the error due to fluorescent quenching effect is not significant in our experiment. In addition, the heating period is carefully controlled less than 20 ms, therefore, the quenching effect is negligible in the measurement.

It is assumed that the sample surface is uniformly heated by laser beam in above analytical solution. However, the laser (405 nm) used in our experiment has a Gaussian intensity profile. To explore the effect of
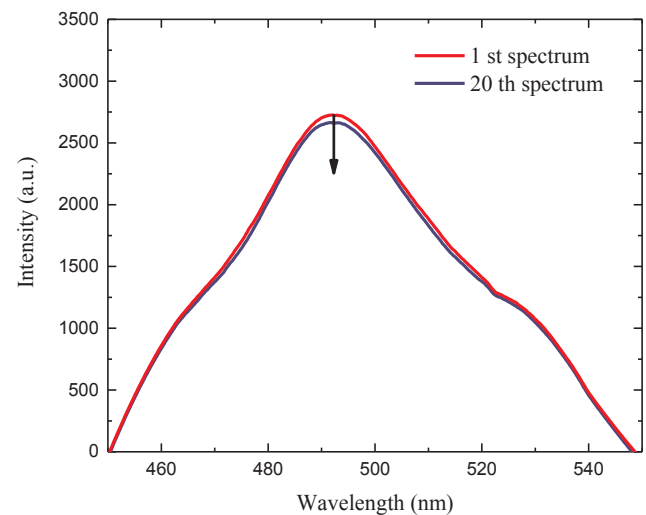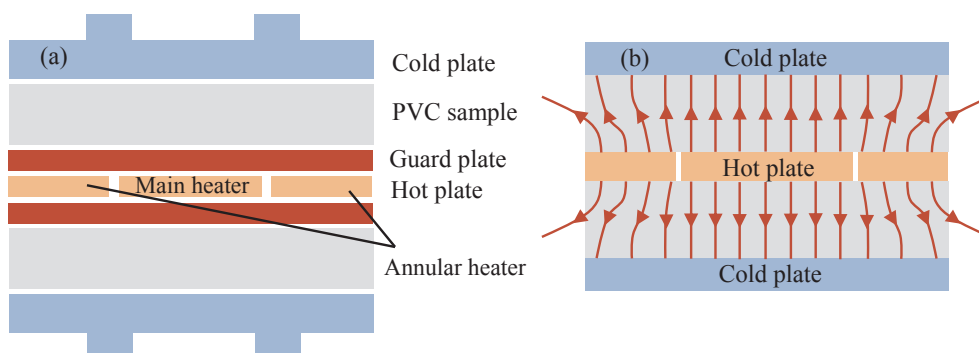

Fig. 4. (a) The classic hot plate apparatus for thermal conductivity measurement of PVC. The sample is clamped between copper plate and cold plate. (b) Heat flux in the sample shows that one-dimensional heat conduction model is applicable. The thermal conductivity of PVC is characterized as 0.19 W/m K.
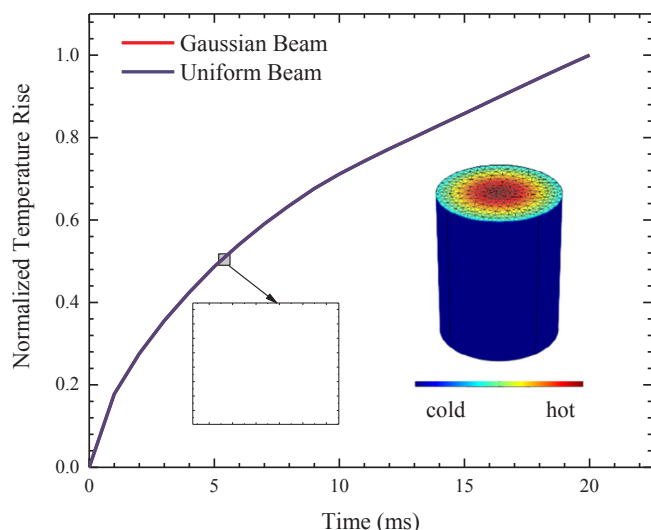
Fig. 6. The simulation results of normalized temperature rise with heating period. The temperature rise is an averaged value across the heating area under both uniform and Gaussian irradiation. The curve of Gaussian laser beam heating result almost overlaps with that of uniform laser beam heating effect. Insert picture shows temperature distribution of sample heated by Gaussian laser beam.

of linear relationship between fluorescence intensity and temperature is $-18.13^{+0.27}_{-0.27}$. Therefore, the excellent linearity and small uncertainty values confirms the accuracy of temperature determination from their correlation. Moreover, the signal noise in fluorescence spectrum (shown in Fig. 2c) could also bring some measurement uncertainty, especially for weak signal cases. To minimize this uncertainty, the spectra were averaged more than 10 times for one case of measurement. The spectrum could be much smoother and the measurement uncertainty can be reduced.

This PVC material usually exhibit poor thermal stability with two distinct decomposition stages. The first stage occurs in the temperature range from 280 °C to 400 °C with an approximate 65% mass loss. The second degradation stage happens at around 400–560 °C corresponding to the chain cracking [34,43]. During the experiment, the maximum temperature rise is around 80 °C, ensuring the thermal stability of sample. Indeed, our technique does not need temperature rise to be significant and thus heating can be kept at a low level. Meanwhile, sample surface is polished to ensure a consistent laser absorption and fluorescence excitation.

The technique developed in this work is suitable for measuring bulk polymers. By employing ultra-fast laser, this new technique can achieve thermophysical measurements of thin films at microscale as long as the thermal relaxation time is far below sample thickness. Besides, for materials without fluorescence excitation, a coating of little dose of fluorescence dyes (e.g. quantum dots) on sample surface would enable the fluorescence excitation and thermal characterization [32,33].

4. Conclusion

In summary, we developed a time-domain transient fluorescence spectroscopy to characterize thermal properties of polymers. Based on the temperature response of fluorescence excitation, this technique employs a pulsed laser for transient heating and fluorescence excitation. A semi-infinite model with normalized temperature and heating time is derived to describe the thermal transport process during periodic laser heating. Thermal diffusivity can be obtained from normalized temperature against heating time. A PVC sample is employed as a benchmark by characterizing its thermal diffusivity as 1.031×10^{-7} m^2/s, in good agreement with reference data. A hot plate method is applied to obtaining thermal conductivity. It is validated that the quenching effect of fluorescence in our measurement can be neglected, and the assumption of uniform laser heating is feasible in physical model derivation. The successful measurement of PVC proves that this time-domain transient fluorescence method can be well applied to polymers. Compared with conventional methods, this new technique is much simpler by employing a single laser. Meanwhile, it doesn't require laser absorption value and temperature coefficient calibration. Since most polymers have excellent fluorescence excitation, this method provides a wide range of application potentials for newly polymer materials.

Appendix A. Supplementary material

Supplementary data associated with this article can be found, in the online version, at http://dx.doi.org/10.1016/j.applthermaleng.2018.04.076.

References

[1] T. Ramanathan, A. Abdala, S. Stankovich, D. Dikin, M. Herrera-Alonso, R. Piner, D. Adamson, H. Schniepp, X. Chen, R. Ruoff, Functionalized graphene sheets for polymer nanocomposites, Nat. Nanotechnol. 3 (2008) 327–331.

[2] T. Kuilla, S. Bhadra, D. Yao, N.H. Kim, S. Bose, J.H. Lee, Recent advances in graphene based polymer composites, Prog. Polym. Sci. 35 (2010) 1350–1375.

[3] Z. Spitalsky, D. Tasis, K. Papagelis, C. Galiotis, Carbon nanotube–polymer composites: chemistry, processing, mechanical and electrical properties, Prog. Polym. Sci. 35 (2010) 357–401.

[4] S. Tsuda, M. Shimizu, F. Iguchi, H. Yugami, Enhanced thermal transport in polymers with an infrared-selective thermal emitter for electronics cooling, Appl. Therm. Eng. 113 (2017) 112–119.

[5] G. Schwartz, B.C.-K. Tee, J. Mei, A.L. Appleton, D.H. Kim, H. Wang, Z. Bao, Flexible polymer transistors with high pressure sensitivity for application in electronic skin and health monitoring, Nat. Commun. 4 (2013) 1859.

[6] J. You, L. Dou, K. Yoshimura, T. Kato, K. Ohya, T. Moriarty, K. Emery, C.-C. Chen, J. Gao, G. Li, A polymer tandem solar cell with 10.6% power conversion efficiency, Nat. Commun. 4 (2013) 1446.

[7] J. Benson, I. Kovalenko, S. Boukhalfa, D. Lashmore, M. Sanghadasa, G. Yushin, Multifunctional CNT-polymer composites for ultra-tough structural supercapacitors and desalination devices, Adv. Mater. 25 (2013) 6625–6632.

[8] E.-C. Cho, J.-H. Huang, J.-P. Li, C.-W. Chang-Jian, K.-C. Lee, Y.-S. Hsiao, J.-H. Huang, Graphene-based thermoplastic composites and their application for LED thermal management, Carbon 102 (2016) 66–73.

[9] X. Liu, Y. Guo, Y. Ma, H. Chen, Z. Mao, H. Wang, G. Yu, Y. Liu, Flexible, low-voltage and high-performance polymer thin-film transistors and their application in photo/thermal detectors, Adv. Mater. 26 (2014) 3631–3636.

[10] G.-H. Kim, D. Lee, A. Shanker, L. Shao, M.S. Kwon, D. Gidley, J. Kim, K.P. Pipe, High thermal conductivity in amorphous polymer blends by engineered interchain interactions, Nat. Mater. 14 (2015) 295–300.

[11] G.-W. Lee, M. Park, J. Kim, J.I. Lee, H.G. Yoon, Enhanced thermal conductivity of polymer composites filled with hybrid filler, Compos. Part A: Appl. Sci. Manuf. 37 (2006) 727–734.

[12] S.H. Song, K.H. Park, B.H. Kim, Y.W. Choi, G.H. Jun, D.J. Lee, B.S. Kong, K.W. Paik, S. Jeon, Enhanced thermal conductivity of epoxy-graphene composites by using non-oxidized graphene flakes with non-covalent functionalization, Adv. Mater. 25 (2013) 732–737.

[13] W.N. dos Santos, P. Mummery, A. Wallwork, Thermal diffusivity of polymers by the laser flash technique, Polym. Test. 24 (2005) 628–634.

[14] X. Wang, V. Ho, R.A. Segalman, D.G. Cahill, Thermal conductivity of high-modulus polymer fibers, Macromolecules 46 (2013) 4937–4943.

[15] S. Xu, T. Wang, D. Hurley, Y. Yue, X. Wang, Development of time-domain differential Raman for transient thermal probing of materials, Opt. Exp. 23 (2015) 10040–10056.

[16] T. Wang, S. Xu, D.H. Hurley, Y. Yue, X. Wang, Frequency-resolved Raman for transient thermal probing and thermal diffusivity measurement, Opt. Lett. 41 (2016) 80–83.

[17] W. Zhao, W. Chen, Y. Yue, S. Wu, In-situ two-step Raman thermometry for thermal characterization of monolayer graphene interface material, Appl. Therm. Eng. 113 (2017) 481–489.

[18] Q. Li, C. Liu, X. Wang, S. Fan, Measuring the thermal conductivity of individual carbon nanotubes by the Raman shift method, Nanotechnology 20 (2009) 145702.

[19] A.A. Balandin, S. Ghosh, W. Bao, I. Calizo, D. Teweldebrhan, F. Miao, C.N. Lau, Superior thermal conductivity of single-layer graphene, Nano Lett. 8 (2008) 902–907.

[20] C. Li, S. Xu, Y. Yue, B. Yang, X. Wang, Thermal characterization of carbon nanotube fiber by time-domain differential Raman, Carbon 103 (2016) 101–108.

[21] A.J. Bur, M.G. Vangel, S. Roth, Temperature dependence of fluorescent probes for applications to polymer materials processing, Appl. Spectrosc. 56 (2002) 174–181.

[22] C. Gota, S. Uchiyama, T. Yoshihara, S. Tobita, T. Ohwada, Temperature-dependent fluorescence lifetime of a fluorescent polymeric thermometer, poly (N-iso-propylacrylamide), labeled by polarity and hydrogen bonding sensitive 4-sulfa-moyl-7-aminobenzofurazan, J. Phys. Chem. B 112 (2008) 2829–2836.

[23] F. Ye, C. Wu, Y. Jin, Y.-H. Chan, X. Zhang, D.T. Chiu, Ratiometric temperature sensing with semiconducting polymer dots, J. Am. Chem. Soc. 133 (2011) 8146.

[24] P. Kujawa, F. Tanaka, F.M. Winnik, Temperature-dependent properties of telechelic hydrophobically modified poly (N-isopropylacrylamides) in water: evidence from light scattering and fluorescence spectroscopy for the formation of stable me-soglobules at elevated temperatures, Macromolecules 39 (2006) 3048–3055.

[25] W. Rettig, B. Strehmel, S. Schrader, H. Seifert, Applied Fluorescence in Chemistry, Biology and Medicine, Springer Science & Business Media, 2012.

[26] K. Okabe, N. Inada, C. Gota, Y. Harada, T. Funatsu, S. Uchiyama, Intracellular temperature mapping with a fluorescent polymeric thermometer and fluorescence lifetime imaging microscopy, Nat. Commun. 3 (2012) 705.

[27] C. Wu, D.T. Chiu, Highly fluorescent semiconducting polymer dots for biology and medicine, Angew. Chem. Int. Ed. 52 (2013) 3086–3109.

[28] P. Bosch, F. Catalina, T. Corrales, C. Peinado, Fluorescent probes for sensing pro-cesses in polymers, Chem.–A Eur. J. 11 (2005) 4314–4325.

[29] Y. Yue, X. Wang, Nanoscale thermal probing, Nano Rev. 3 (2012) 11865.

[30] I. Sedmak, I. Urbančič, J. Štrancar, M. Mortier, I. Golobič, Transient submicron temperature imaging based on the fluorescence emission in an Er/Yb co-doped glass–ceramic, Sens. Actu., A 230 (2015) 102–110.

[31] J.S. Donner, S.A. Thompson, M.P. Kreuzer, G. Baffou, R. Quidant, Mapping in-tracellular temperature using green fluorescent protein, Nano Lett. 12 (2012) 2107–2111.

[32] O. Yarimaga, S. Lee, D.Y. Ham, J.M. Choi, S.G. Kwon, M. Im, S. Kim, J.M. Kim, Y.K. Choi, Thermofluorescent conjugated polymer sensors for nano-and microscale temperature monitoring, Macromol. Chem. Phys. 212 (2011) 1211–1220.

[33] X. Wan, C. Li, Y. Yue, D. Xie, M. Xue, N. Hu, Development of steady-state electrical-heating fluorescence-sensing (SEF) technique for thermal characterization of one dimensional (1D) structures by employing graphene quantum dots (GQDs) as temperature sensors, Nanotechnology 27 (2016) 445706.

[34] J. Yu, L. Sun, C. Ma, Y. Qiao, H. Yao, Thermal degradation of PVC: a review, Waste Manage. (Oxford) 48 (2016) 300–314.

[35] C. Choy, Thermal conductivity of polymers, Polymer 18 (1977) 984–1004.

[36] D. Salmon, Thermal conductivity of insulations using guarded hot plates, including recent developments and sources of reference materials, Meas. Sci. Technol. 12 (2001) R89.

[37] P. Bonnet, D. Sireude, B. Garnier, O. Chauvet, Thermal properties and percolation in carbon nanotube-polymer composites, Appl. Phys. Lett. 91 (2007) 201910.

[38] W.M. Haynes, CRC Handbook of Chemistry and Physics, CRC Press, 2014.

[39] W.N. dos Santos, Thermal properties of polymers by non-steady-state techniques, Polym. Test. 26 (2007) 556–566.

[40] L. Chen, D.W. McBranch, H.-L. Wang, R. Helgeson, F. Wudl, D.G. Whitten, Highly sensitive biological and chemical sensors based on reversible fluorescence quenching in a conjugated polymer, Proc. Natl. Acad. Sci. 96 (1999) 12287–12292.

[41] C. Fan, K.W. Plaxco, A.J. Heeger, High-efficiency fluorescence quenching of con-jugated polymers by proteins, J. Am. Chem. Soc. 124 (2002) 5642–5643.

[42] B. Liu, Y. Bao, H. Wang, F. Du, J. Tian, Q. Li, T. Wang, R. Bai, An efficient con-jugated polymer sensor based on the aggregation-induced fluorescence quenching mechanism for the specific detection of palladium and platinum ions, J. Mater. Chem. 22 (2012) 3555–3561.

[43] H. Zhu, X. Jiang, J. Yan, J. Chi, K. Cen, TG-FTIR analysis of PVC thermal de-gradation and HCl removal, J. Anal. Appl. Pyrol. 82 (2008) 1–9.